American Mineralogist, Volume 79, pages 161–167, 1994

S speciation in submarine basaltic glasses as determined by measurements of S$K\alpha$ X-ray wavelength shifts

Paul J. Wallace
Department of the Geophysical Sciences, University of Chicago, Chicago, Illinois 60637, U.S.A.
Ian S. E. Carmichael
Department of Geology and Geophysics, University of California at Berkeley, Berkeley, California 94720, U.S.A.

Abstract

S occurs in both oxidized (S^{6+}) and reduced (S^{2-}) forms in natural silicate liquids. The wavelength of S$K\alpha$ radiation changes as a function of the oxidation state of S and can be used to determine the proportions of sulfide and sulfate in unknown samples by comparison with reference standards of a known valence state. We have measured the wavelength of S$K\alpha$ X-rays in a variety of glassy submarine lavas from spreading centers (Juan de Fuca, Galápagos, Kane, and Southeast Indian Ridge), seamounts (Loihi and Lamont seamounts), and back-arc basins (Lau Basin). The relative f_{O_2} values of these glasses are known from wet-chemical determinations of FeO and Fe_2O_3 and vary from slightly above the Ni + NiO buffer (NNO) to 3.2 log units below NNO. Measured values of sulfate/S_{tot} (S^{6+}/S_{tot}) vary from 0.02 to 0.25 and increase with increasing relative f_{O_2}. Our results demonstrate that the dissolved S in these samples occurs predominately as S^{2-}. Large variations in H_2O content have no measurable effect on the redox state of S, suggesting that H_2S or HS^- are not abundant S species in solution in silicate liquids. Thermodynamic calculations show that the speciation of S in coexisting gas during submarine eruptions of basaltic magma is also dependent on relative f_{O_2}. Many lavas from seamounts and back-arc basins are predicted to have S present mainly as SO_2 in coexisting magmatic gas, whereas the lower f_{O_2} of midocean ridge basalts favor H_2S as the dominant form of gaseous S.

Introduction

S occurs in silicate liquids as both reduced (S^{2-}) and oxidized (S^{6+}) species, and the relative proportions of the two appear to be largely controlled by the oxidation state of the liquid (Fincham and Richardson, 1954; Connolly and Haughton, 1972; Nagashima and Katsura, 1973; Katsura and Nagashima, 1974; Carroll and Rutherford, 1988). The effects of other factors such as temperature, pressure, bulk composition, and H_2O content on the S redox state and speciation are not clear but are important for understanding the stability of S-bearing minerals, sulfide liquid immiscibility, and degassing of S species from active volcanoes. The proportions of oxidized and reduced S (S^{6+}/S_{tot}) in quenched silicate liquids can be measured by the X-ray spectrometric technique of Carroll and Rutherford (1988). This technique is based on the wavelength shift of S$K\alpha$ radiation that is caused by variation in the S valence state and its effect on bond energies (Wilbur and Gofman, 1965).

Using this technique, we have measured (S^{6+}/S_{tot}) in 22 rapidly quenched, submarine glasses from a variety of tectonic settings, including spreading centers, propagating ridges, seamounts, and back-arc basins. In our previous work (Wallace and Carmichael, 1992a), we estimated preeruptive equilibration temperatures and the f_{O_2}, f_{S_2}, and f_{SO_2} for these samples, which allowed us also to examine any effects that variations in these intensive parameters may have on the S redox state. Our results provide new data on the speciation of S in basaltic magmas and the solution mechanisms by which sulfide dissolves in silicate liquids. Combined with thermodynamic calculations of the speciation of S in a coexisting gas phase, these results provide constraints on the effects of S loss during eruptions of basaltic magma.

Analytical methods

The glass samples analyzed in this study are largely basaltic and span a wide range of bulk composition, magmatic f_{O_2}, S_{tot} content, and preeruptive equilibration temperature. They include nepheline-normative alkali basalts, tholeiites, highly differentiated Fe- and Ti-rich basalts, and several andesites from the Lau Basin. Details concerning the major-element compositions of these glasses (except for the Lau Basin samples, which are given in the appendix) are presented in Wallace and Carmichael (1992a), along with information regarding FeO analyses and the calculation of relative f_{O_2}.

Measurements of the wavelength of S$K\alpha$ radiation [λ(S$K\alpha$)] for the glass samples were conducted using both an eight-channel ARL SEMQ electron microprobe at the

0003–004X/94/0102–0161$02.00

TABLE 1. Measured S$K\alpha$ wavelength shifts for sulfide and sulfate standards

	Anhydrite*	Anhydrite**	Barite**	Pyrite**
$\Delta\lambda(SK\alpha)$ (Å × 10^3)	3.00	3.07	3.20	0.51
	3.03	3.07	3.05	0.39
	2.98	3.04		0.58
		3.26		0.41
		3.06		0.24
		3.14		0.30
		2.94		0.38
		3.09		0.27
Average	3.00	3.08	3.13	0.39
Standard deviation	0.03	0.09	0.11	0.12

Note: $\Delta\lambda(SK\alpha)$ is the S$K\alpha$ wavelength shift measured relative to FeS in units of ångströms times 10^3.

* Measured at University of Chicago with Cameca SX-50.

** Measured at University of California at Berkeley with ARL-SEMQ.

University of California at Berkeley and a four-channel Cameca SX-50 electron microprobe at the University of Chicago. With the former instrument, analyses were performed using ADP and PET crystals on two spectrometers, allowing two independent measurements to be made simultaneously, whereas the Cameca SX-50 was equipped with PET crystals on each of three spectrometers. Analyses performed with the two instruments yielded similar results. Operating conditions were an accelerating voltage of 15 kV, a beam current of 25–30 nA, a beam diameter of 10 μm, and a counting time of 20–40 s per spot for the glass samples and 5–10 s for the standards. Following the techniques of Carroll and Rutherford (1988), measurements of $\lambda(SK\alpha)$ in FeS were performed before and after each unknown, and all wavelength shifts are calculated relative to this standard. For each wavelength scan the spectrometers were moved through a total range of 0.005 sin θ units in 100 steps of 0.00005 sin θ units per step. For the glass samples the electron beam must be moved to a new spot after each step in the scan. Leaving the electron beam in a single spot longer than about 15 min causes an apparent increase in $\lambda(SK\alpha)$ of the sample relative to FeS (Wallace and Carmichael, 1992b), perhaps due to electron beam damage of the glass, diffusion in the sample and consequent charge-balance effects, or charge build-up. Reference samples containing S of known valence state are similar to those employed by Carroll and Rutherford (1988) and include Canyon Diablo troilite and pyrrhotite (FeS) for S^{2-} and anhydrite ($CaSO_4$) for S^{6+}. In addition we have measured S$K\alpha$ wavelength shifts for pyrite (FeS_2) and barite ($BaSO_4$).

For each sample, $\lambda(SK\alpha)$ was determined by fitting the wavelength scan data with a Gaussian function to estimate the S$K\alpha$ peak center, from which the wavelength can be calculated using Bragg's law. Average values for wavelength shifts relative to FeS [$\Delta\lambda(SK\alpha)$] for the standards are listed in Table 1, and for the glass samples, in Table 2. The total S$K\alpha$ wavelength shift between sulfide and sulfate for both anhydrite and barite agree within error and are consistent with previous determinations (Carroll and Rutherford, 1988). The value of $\Delta\lambda(SK\alpha)$ for pyrite (S^-) is approximately ⅛ of the total shift between S^{2-} and S^{6+}, consistent with a linear increase of S$K\alpha$ energy with an increasing S valence state (Kucha et al., 1989).

TABLE 2. Measured S$K\alpha$ wavelength shifts for submarine glassy lavas

Sample	ΔNNO	$\Delta\lambda(SK\alpha)$ (Å × 10^3)	S^{6+}/S_{tot}	S (ppmw)	S^{6+}	S^{2-}
Kane fracture zone						
TK-6-12	−2.0	0.17 ± 0.01	0.06 ± 0.01	1050	60	990
TK-2-12	−2.4	0.10 ± 0.02	0.03 ± 0.01	1000	35	965
TK-14	−3.2	0.13 ± 0.05	0.04 ± 0.02	1100	50	1050
Southeast Indian Ridge						
V33-D1-2	−2.6	0.05 ± 0.03	0.02 ± 0.01	1250	20	1230
Juan de Fuca Ridge						
D1-4	−1.2	0.16 ± 0.02	0.05 ± 0.01	1800	95	1705
Galápagos Spreading Center 85.5°W						
997-4	−0.5	0.13 ± 0.04	0.04 ± 0.02	2400	100	2300
996-6	−0.6	0.22 ± 0.02	0.07 ± 0.01	2250	165	2085
996-5	−0.9	0.17 ± 0.10	0.06 ± 0.03	2450	140	2310
996-8	−1.5	0.17 ± 0.10	0.06 ± 0.03	2350	135	2215
Galápagos Spreading Center 95.5°W						
1540-4	−0.3	0.21 ± 0.19	0.07 ± 0.06	1250	90	1160
1557-3	−1.8	0.08 ± 0.05	0.03 ± 0.02	1300	35	1265
Lamont seamounts						
1560-1843Z	−0.1	0.28 ± 0.11	0.09 ± 0.04	1100	105	995
1560-1922	−1.3	0.16 ± 0.14	0.05 ± 0.05	1100	60	1040
Loihi seamount						
KK-15-4	0.0*	0.64 ± 0.13	0.21 ± 0.05	1850	395	1455
KK-15-5	−1.1	0.11 ± 0.04	0.04 ± 0.01	1050	40	1010
KK-19-21	−1.6	0.13 ± 0.03	0.04 ± 0.01	1800	80	1720
KK-29-10	−2.4	0.13 ± 0.13	0.04 ± 0.04	1250	55	1195
Lau Basin						
20-5-1	0.3	0.75 ± 0.12	0.25 ± 0.05	650	165	485
12-5-3	0.2	0.49 ± 0.05	0.16 ± 0.03	700	115	585
10-1-3	−0.4	0.19 ± 0.18	0.06 ± 0.06	1900	120	1780
41-3-2	−0.8	0.07 ± 0.05	0.02 ± 0.07	750	20	730
22-6-2	−1.6	0.06 ± 0.06	0.02 ± 0.02	1050	20	1030

Note: ΔNNO is the f_{O_2} of the sample relative to the Ni + NiO buffer. Data for ΔNNO and S abundances (in parts per million by weight) are from Wallace and Carmichael (1992a). The $\Delta\lambda(SK\alpha)$ is the S$K\alpha$ wavelength shift and uncertainty (1σ) of the sample relative to FeS. Values for S^{6+}/S_{tot} are calculated from $\Delta\lambda(SK\alpha)$, following the method described in the text, and allow calculation of the concentrations (in parts per million by weight) of S^{6+} and S^{2-} from the S_{tot} abundance. Uncertainties (1σ) for S^{6+}/S_{tot} include propagation of uncertainty in $\Delta\lambda(SK\alpha)$ for anhydrite. Sample locations and additional data for samples from each of the numbered regions can be found in Wallace and Carmichael (1992a) and the following sources: (1) Langmuir and Bender (unpublished data); (2) Klein et al. (1991); (3) Kappel (unpublished data); (4) Fornari et al. (1983); (5) Christie and Sinton (1981); (6) Allan et al. (1989); (7) Frey and Clague (1983); (8) Appendix Table 1 and Pearce (unpublished data).

* This value is higher, but within error, of the value (−0.4) previously reported in Wallace and Carmichael (1992a) and is based on three replicate analyses that yielded an FeO content of 9.46 wt%.

RESULTS

The measured values of $\Delta\lambda(SK\alpha)$ for the glasses in Table 2 are shown in Figure 1 as a function of relative magmatic f_{O_2}. They vary from 0.05 × 10^{-3} to 0.75 × 10^{-3} Å, all of which are small compared with the total wavelength shift between sulfide (S^{2-}) and sulfate (3 × 10^{-3} Å). For f_{O_2} between 3.2 and 0.1 log units below NNO (ΔNNO = −3.2 to −0.1), $\Delta\lambda(SK\alpha)$ remains relatively constant, showing a slight overall increase with increasing ΔNNO. Three of the most oxidized samples have significantly higher values.

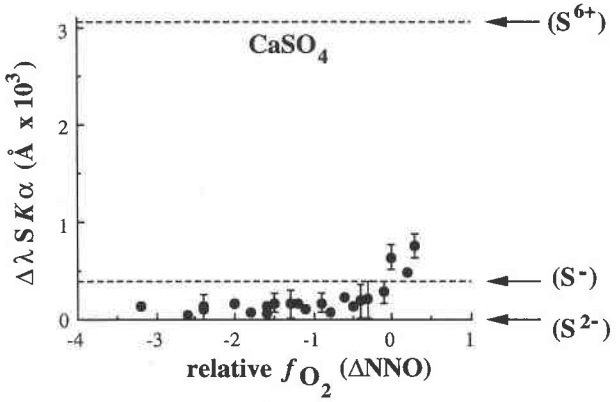

Fig. 1. S$K\alpha$ wavelength shifts measured relative to FeS plotted against relative f_{O_2} (ΔNNO). Dashed lines show Δλ(S$K\alpha$) for anhydrite (S^{6+}) and pyrite (S^-). Error bars, where shown, give the standard deviation (1σ) of the measurement. For other samples the error is smaller than the symbol size.

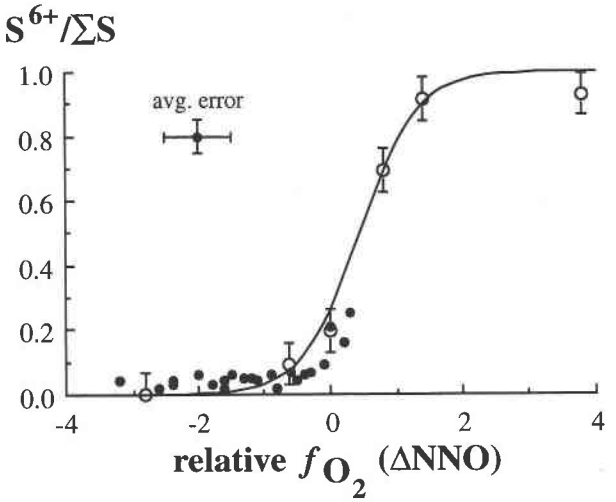

Fig. 2. Data for S^{6+}/S_{tot} plotted against relative f_{O_2} (ΔNNO) for glasses in Table 2 (solid circles) and the experimental glasses (open circles) of Carroll and Rutherford (1988). Representative error for our measurements is shown in the upper left, whereas those for the experimental glasses are shown with the symbol (open circles). Solid line is calculated using Eq. 4.

In order to interpret the wavelength shift data as a quantitative determination of the proportion of oxidized S (S^{6+}/S_{tot}), we have assumed that Δλ(S$K\alpha$) increases linearly with S^{6+}/S_{tot}. Carroll and Rutherford (1988) have demonstrated that this assumption gives results that agree with the data of Nagashima and Katsura (1973) and Katsura and Nagashima (1974). In these last two studies, melts equilibrated at known f_{O_2} values were analyzed for sulfide and sulfate using wet-chemical methods. It should also be noted that we are assuming that all of the S occurs as S^{2-} and S^{6+}. The data shown in Figure 1 clearly indicate that a substantial amount of S occurs as S^{2-} because all but a few of the most oxidized samples have Δλ(S$K\alpha$) $< 0.3 \times 10^{-3}$ Å, smaller than the value for S^- of 0.39×10^{-3} Å determined by analyzing pyrite (Table 1). In principle the Δλ(S$K\alpha$) data for these samples could be interpreted as being a mixture of S^{2-} and S^-, but the vacuum distillation analyses of Sakai et al. (1984) for basalt glass samples of similar f_{O_2} show that some sulfate is also present under these conditions. Their data are consistent with our results only if most or all of the reduced S occurs as S^{2-}. Similarly, the data of Carroll and Rutherford (1988) for samples equilibrated at high f_{O_2} show that most of the S occurs as S^{6+}, although the presence of some sulfite (S^{4+}), especially at intermediate f_{O_2}, cannot be ruled out. Thus the S$K\alpha$ wavelength shift and vacuum distillation data are consistent with S^{2-} and S^{6+} as the major forms of dissolved S in silicate liquids. If some sulfite is present, it will not significantly affect our estimates of the proportions of oxidized and reduced S because S^{4+} has Δλ(S$K\alpha$) much closer to that of sulfate (S^{6+}) than to S^{2-} (Kucha et al., 1989).

Calculated values of S^{6+}/S_{tot} for the submarine glasses vary from 0.02 to 0.25 (Table 2), indicating that the majority of the S in these samples is present as S^{2-}. These data are plotted in Figure 2 as a function of the relative f_{O_2} of the sample. Shown for reference are the data of Carroll and Rutherford (1988) for glasses that were equilibrated at known f_{O_2} values. Our data for submarine glasses are in excellent agreement with the relationship that they found between relative f_{O_2} and S^{6+}/S_{tot}. This is significant, given the large differences in H_2O contents, bulk compositions, and equilibration temperatures between the two sample sets. Calculated equilibration temperatures for the submarine glasses vary from 1250 to 1055 °C, whereas the experimental glasses were largely equilibrated at temperatures between 1025 and 920 °C. Within the range of our data, there are no other consistent relationships between S^{6+}/S_{tot} and other variables (e.g., temperature, Fe content, silica activity). There is some correlation of S^{6+}/S_{tot} with f_{S_2} and f_{SO_2}, but this is probably due to the relationships among f_{S_2}, f_{SO_2}, and f_{O_2} for basaltic melts that are saturated with immiscible monosulfide Fe-S-O liquid (Wallace and Carmichael, 1992a). Therefore we conclude that f_{O_2} is the dominant parameter controlling S^{6+}/S_{tot} in silicate liquids and that other variables have no measurable effect. Carroll and Rutherford (1988) arrived at the same conclusions on the basis of their experimental data, and our new results extend this relationship over a wider range of compositions and temperatures.

Discussion

Sulfide-sulfate equilibrium in silicate liquids

The S oxidation reaction in silicate liquids can be expressed as

$$S^{2-}_{melt} + 2O_{2(gas)} = SO^{2-}_{4melt} \quad (1)$$

with

$$K_1 = a_{SO_4^{2-}\,melt}/a_{S^{2-}_{melt}} \cdot f_{O_2}^2. \quad (2)$$

If the ratio of the activity coefficients modifying the mole fractions (X) remains constant, then the sulfate to sulfide ratio in silicate liquids can be represented by

$$\log(X_{SO_4^{2-}}/X_{S^{2-}}) = \log K + 2 \log f_{O_2} \quad (3)$$

where K is modified from Equation 2 to incorporate the activity coefficients. The data of Carroll and Rutherford (1988) show that the ratio $X_{SO_4^{2-}}/X_{S^{2-}}$ (which can be calculated from S^{6+}/S_{tot}) is dependent on the relative f_{O_2}, suggesting that the temperature dependence of K_1 is similar to that of other redox reactions such as Ni + NiO (NNO) or fayalite + magnetite + quartz (FMQ). Using linear regression their data can be fitted to an expression based on Equation 3:

$$\log(X_{SO_4^{2-}}/X_{S^{2-}}) = a \log f_{O_2} + b/T + c \quad (4)$$

where $a = 1.02$, $b = 25410$ K, and $c = -10.0$. The temperature coefficient (b) is taken from the Ni + NiO reaction (Huebner and Sato, 1970), multiplied by 1.02, so that $X_{SO_4^{2-}}/X_{S^{2-}}$ is only dependent on relative f_{O_2}. We also note that the value for a is considerably lower than the value of 2 predicted by Equation 3.

Values of S^{6+}/S_{tot} calculated from Equation 4 are shown in Figure 2. The calculated values fit most of the experimental and natural data within error, although it appears that at high and low f_{O_2}, Equation 4 may slightly overestimate and underestimate, respectively, the actual value of S^{6+}/S_{tot}. This may indicate that the ratio of the activity coefficients of SO_4^{2-} and S^{2-} does not remain constant over the entire range of f_{O_2}, or that $\log(X_{SO_4^{2-}}/X_{S^{2-}})$ is not a simple linear function of $\log f_{O_2}$ (i.e., the a coefficient varies with relative f_{O_2}).

The relationship of S^{6+}/S_{tot} to relative f_{O_2} makes it possible to estimate relative magmatic f_{O_2} using Equation 4, together with measured values of $SK\alpha$ wavelength shifts. S^{6+}/S_{tot} changes rapidly over the interval from NNO − 1 to NNO + 2, making it a sensitive indicator of f_{O_2} for samples in this range. As an example, it may be possible to use this method on glass inclusions in phenocrysts from volcanic rocks for which other means of estimating f_{O_2} (e.g., Fe-Ti oxides or Fe_2O_3/FeO analysis) are not suitable.

Role of H_2O in S speciation

Measurements of S^{6+}/S_{tot} in silicate glasses provide constraints on the speciation of S in magmas and the mechanisms by which these species dissolve. Of particular importance is the role of H_2O in the dissolution of sulfide in hydrous melts. One possibility is that sulfide dissolves by forming H_2S or HS^- through equilibria such as

$$H_2O_{melt} + SO_{3\,melt} = H_2S_{melt} + 2O_{2\,gas} \quad (5a)$$

$$OH^-_{melt} + SO_{3\,melt} = HS^-_{melt} + 2O_{2\,gas}. \quad (5b)$$

These equilibria predict that at constant f_{O_2}, increases in H_2O content should increase the proportion of sulfide (present as H_2S or HS^-) by reduction of S^{6+} in the melt. H_2O contents for glasses from the same regions and of the same general compositions as our samples are commonly <0.5 wt% H_2O (Muenow et al., 1990, and references therein), but in some (e.g., Lau Basin), the H_2O content may be as high as 1.5 wt%. In contrast, the compositions investigated by Carroll and Rutherford (1988) were chosen to be representative of the types of H_2O-rich magmas that erupt along continental margins and were equilibrated at H_2O-saturated conditions at pressures of 1–4.5 kbar. The total range of H_2O contents covered by their data set and ours translate into variations in f_{H_2O} that range over three orders of magnitude and should cause large increases in the amount of reduced S if H_2S or HS^- are abundant sulfide species in silicate melts. Instead, within the precision of the S^{6+}/S_{tot} data (ca. 10–15% absolute), there is no measurable effect.

An alternative to Equations 5a and 5b is that S^{2-} dissolves in silicate liquids by forming a complex with Fe through equilibria such as

$$CaSO_{4\,melt} + FeO_{melt} = FeS_{melt} + CaO_{melt} + 2O_{2\,gas} \quad (6a)$$

$$SO^{2-}_{4\,melt} = S^{2-}_{melt} + 2O_{2\,gas}. \quad (6b)$$

Under reducing conditions, where sulfide is the dominant S species, it has been demonstrated experimentally in anhydrous silicate liquids that increases in Fe content cause an increase in the amount of S that dissolves, which is likely to be caused by the formation of a complex of Fe^{2+} and S^{2-} (Haughton et al., 1974). At high f_{O_2} values, where oxidized S is the dominant S species, anhydrite precipitates from S-saturated silicate liquids (Carroll and Rutherford, 1985, 1987; Luhr, 1990), suggesting that $CaSO_4$ may be an important melt species for sulfate. Other network-modifying cations are probably also involved to a lesser extent in the formation of sulfide and sulfate complexes in silicate liquids. If Equation 6a is applicable, then variations in a_{FeO} should also have an effect on S^{6+}/S_{tot}. Although the samples in Table 2 cover a wide range of FeO contents (7.3–15.8 wt%), the consequent values of a_{FeO} for this range vary only by a factor of 2 (calculated from Snyder and Carmichael, 1992), and therefore, any effect of a_{FeO} would be much less than that caused by variations in f_{H_2O}. No correlation is observed between a_{FeO} and S^{6+}/S_{tot} for the data in Table 2, but that is not surprising, given the small range of variations in a_{FeO} and the errors of the S^{6+}/S_{tot} measurements. In conclusion, with the absence of a measurable effect of large variations in f_{H_2O} on the redox state of S, it seems probable that H_2S or HS^- are not abundant species by which sulfide dissolves in silicate liquids.

Fugacities of S species in basaltic magmas and the effects of degassing

Basaltic magmas are typically saturated with CO_2-rich gas during ascent and eruption on the sea floor (Moore et al., 1977). Although the dominant forms of dissolved S in silicate liquids are S^{2-} and S^{6+}, the S species that are

present in coexisting magmatic gas are H_2S, S_2, and SO_2. The fugacities of these species are related through the following equilibria:

$$0.5S_2 + O_2 = SO_2 \quad (7)$$

$$H_2S + 1.5O_2 = SO_2 + H_2O. \quad (8)$$

Thus the values of f_{H_2S}, f_{S_2}, and f_{SO_2} are dependent not only on temperature and pressure, but also on f_{O_2} and f_{H_2O}. Even though H_2S is not an abundant melt species, it may be a significant component of the gas, especially at high f_{H_2O} or low f_{O_2} (Eq. 8). Values of f_{H_2O} for basaltic magmas can be calculated from magmatic H_2O contents using the methods of Dixon (1992). Most midocean ridge basalts (MORB) contain $\leq$0.4 wt% H_2O (Muenow et al., 1990), whereas the lavas of Loihi seamount contain 0.3–0.8 wt% (Byers et al., 1985), and those of the Lau Basin may contain as much as 1.0 wt% or more (Aggrey et al., 1988). It is important to note that at pressures relevant to submarine eruptions of basaltic magma ($\leq$500 bars) f_{H_2O} is not dependent on pressure (Dixon, 1992), and therefore, at a given f_{O_2} and H_2O content, f_{SO_2}/f_{H_2S} calculated from Equation 8 will not vary as a function of pressure.

Shown in Figure 3 are values of $\log(f_{SO_2}/f_{H_2S})$ in a coexisting magmatic gas phase at 1200 °C calculated as a function of magmatic H_2O content and relative f_{O_2}. SO_2 is the major S species for basaltic magmas that are more oxidized than FMQ (NNO − 0.7) and contain $\leq$1.0 wt% H_2O, conditions that are appropriate for many lavas from seamounts and back-arc basins (Fig. 3). Under the more reducing conditions that are typical of MORB, H_2S is the dominant S species in the coexisting gas, even for magmas with very low H_2O contents (e.g., 0.1 wt% H_2O and f_{O_2} below NNO − 2). Similar calculations using Equation 7 demonstrate that for low magmatic H_2O contents, S_2 is an important species between NNO − 2 and NNO − 1. As an example, a magma with 0.1 wt% H_2O at 1200 °C and NNO − 2 will have approximately equal proportions of SO_2, H_2S, and S_2 in coexisting gas. Decreasing temperature at constant relative f_{O_2} shifts Equation 8 to the left, as does increasing f_{H_2O}, so that lower temperature H_2O-rich magmas such as andesites and rhyolites have lower f_{SO_2}/f_{H_2S} than the values depicted in Figure 3.

During submarine eruptions of basaltic magma, S is not strongly partitioned into the coexisting gas phase (Moore, 1970; Moore and Schilling, 1973), but, during low-pressure eruptions (subaerial and shallow submarine), extensive loss of S occurs by degassing. For basaltic magmas in the f_{O_2} range between NNO − 1 and NNO + 1 the gas phase SO_2/H_2S ratio is much higher than the melt phase S^{6+}/S^{2-} ratio (Figs. 2 and 3). For example, S is lost predominately as SO_2 from basaltic magmas at Kilauea volcano because at f_{O_2} values between FMQ and NNO the molar ratio SO_2/H_2S in high-temperature volcanic gases is typically >100 (Gerlach, 1980).

Loss of gas with $SO_2/H_2S \gg 1$ may decrease the f_{O_2} of the magma through a reaction proposed by Anderson and Wright (1972):

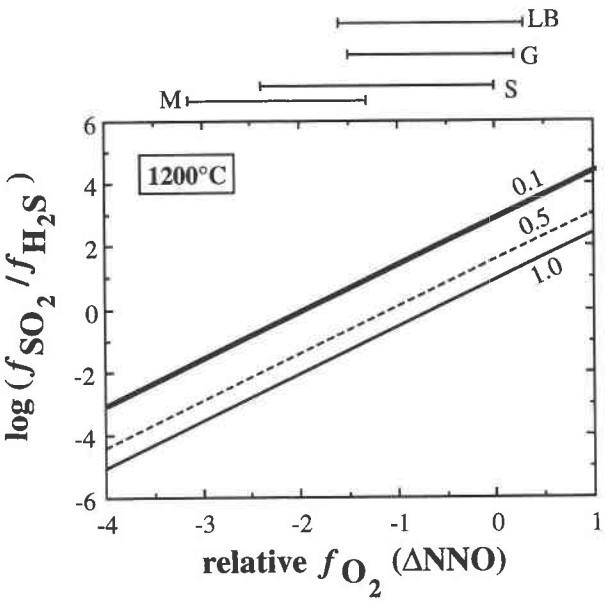

Fig. 3. Log f_{SO_2}/f_{H_2S} in coexisting gas phase at 1200 °C calculated as a function of relative f_{O_2} for basalts with H_2O contents of 0.1 (heavy solid line), 0.5 (dashed line), and 1.0 wt% (light solid line) and at pressures relevant to the eruption of seafloor lavas ($\leq$500 bars). At these pressures, fugacity coefficients for SO_2 and H_2S calculated with the modified Redlich-Kwong equation are close to 1 so that f_{SO_2}/f_{H_2S} is equal to molar SO_2/H_2S of the gas. The equilibrium constant for Eq. 8 has been determined using thermochemical data of Chase et al. (1985). Values of f_{H_2O} have been calculated from Dixon (1992). Horizontal lines indicate the range of relative f_{O_2} for lavas from the following regions: (LB) Lau Basin; (G) Galápagos 85.5°W; (S) Loihi and Lamont seamounts; and (M) midocean ridge basalts. Data from Christie et al. (1986) and Wallace and Carmichael (1992a).

$$FeS_{melt} + 3Fe_2O_{3\,melt} = 7FeO_{melt} + SO_{2\,gas}. \quad (9)$$

Analyses of volcanic gases from Kilauea volcano have very constant relative f_{O_2} values (between FMQ and NNO) over a wide range of temperature and gas composition (Gerlach, 1993). Fe_2O_3/FeO ratios of glassy, basaltic scoria samples from Kilauea indicate f_{O_2} values consistent with the gas analyses (unpublished data) and show no evidence of reduction caused by loss of SO_2. The data of Sakai et al. (1982) showed that many degassed (S $\leq$ 150 ppm) subaerial basalts at Kilauea, including fountain spatter and glassy lavas, have S^{6+}/S_{tot} comparable to undegassed, submarine lavas, which also suggests that SO_2 loss does not significantly affect magmatic f_{O_2}. The majority of S dissolved in Kilauea basaltic magmas is S^{2-} and must be oxidized during degassing by some mechanism other than Equation 9. Gerlach (1993) has shown that the f_{O_2} of Kilauea volcanic gases is buffered by coexisting lava through O transfer and that this transfer controls the f_{SO_2}, f_{S_2}, and f_{H_2S}. Numerous heterogeneous reactions involving C-O-H-S species occur during cooling and degassing of basaltic magmas (Gerlach, 1993), but the evidence from gas analyses and from Fe^{3+}/Fe_{tot} and

S^{6+}/S_{tot} of subaerial Kilauea lavas suggests that these reactions do not cause significant changes in relative f_{O_2} of either gas or lava.

Conclusions

Measured values of S^{6+}/S_{tot} vary from 0.02 to 0.25 and increase with increasing relative f_{O_2} in accordance with the experimentally derived relationship of Carroll and Rutherford (1988). S^{6+}/S_{tot} can be used to estimate f_{O_2} for glassy lavas that are in the range from NNO − 1 to NNO + 2.

Dissolved S in these samples occurs predominately as S^{2-}. Large variations in H_2O content and f_{H_2O} have no measurable effect on the redox state of S, suggesting that H_2S or HS^- are not abundant in silicate liquids.

Thermodynamic calculations of S speciation in coexisting gas during submarine eruptions of basaltic magma show that S may be present mainly as H_2S or SO_2, depending largely on magmatic f_{O_2}. Many lavas from seamounts and back-arc basins are predicted to have molar $SO_2/H_2S > 1$ in coexisting magmatic gas, whereas the lower f_{O_2} values of midocean ridge basalts favor H_2S as the dominant form of gaseous S.

Acknowledgments

We would like to thank the following people for kindly providing the samples used in this study and access to unpublished data: J. Pearce (Lau Basin), E. Kappel and E. Klein (Southeast Indian and Juan de Fuca Ridges), C. Langmuir and J. Bender (Kane fracture zone), M. Perfit and D. Fornari (Galápagos 85°W), D. Clague (Loihi seamount), D. Christie (Galápagos 95°W), and J. Allan (Lamont seamounts). We would also like to thank D. Christie and J. Allan for preparing many of the samples and J. Donovan and I. Steele for assistance with the electron microprobes. Reviews by J. Luhr and M. Rutherford and discussions with A.T. Anderson, Jr., and D. Snyder led to significant improvements. This research was supported in part by National Science Foundation grant EAR-91-05231. P.W. acknowledges the financial support of A.T. Anderson, Jr., during the final stages of this work.

References cited

Aggrey, K.E., Muenow, D.W., and Sinton, J.M. (1988) Volatile abundances in submarine glasses from the North Fiji and Lau back-arc basins. Geochimica et Cosmochimica Acta, 52, 2501–2506.

Allan, J.F., Batiza, R., Perfit, M.R., Fornari, D.J., and Sack, R.O. (1989) Petrology of lavas from the Lamont Seamount Chain and adjacent East Pacific Rise, 10°N. Journal of Petrology, 30, 1245–1298.

Anderson, A.T., and Wright, T.L. (1972) Phenocrysts and glass inclusions and their bearing on oxidation and mixing of basaltic magmas, Kilauea Volcano, Hawaii. American Mineralogist, 57, 188–216.

Byers, C.D., Garcia, M.O., and Muenow, D.W. (1985) Volatiles in pillow rim glasses from Loihi and Kilauea volcanoes, Hawaii. Geochimica et Cosmochimica Acta, 49, 1887–1896.

Carroll, M.R., and Rutherford, M.J. (1985) Sulfide and sulfate saturation in hydrous silicate melts. Journal of Geophysical Research, 90, C601–C612.

——— (1987) The stability of igneous anhydrite: Experimental results and implications for sulfur behaviour in the 1982 El Chichón trachyandesite and other evolved magmas. Journal of Petrology, 28, 781–801.

——— (1988) Sulfur speciation in hydrous experimental glasses of varying oxidation state: Results from measured wavelength shifts of sulfur X-rays. American Mineralogist, 73, 845–849.

Chase, M.W., Jr., Davies, C.A., Downey, J.R., Jr., Frurip, D.J., McDonald, R.A., and Syverud, A.N. (1985) JANAF thermochemical tables (3rd edition). Journal of Physical and Chemical Reference Data, 14, 1856 p.

Christie, D.M., and Sinton, J.M. (1981) Evolution of abyssal lavas along propagating segments of the Galapagos center. Earth and Planetary Science Letters, 56, 321–335.

Christie, D.M., Carmichael, I.S.E., and Langmuir, C.H. (1986) Oxidation states of mid-ocean ridge basalt glasses. Earth and Planetary Science Letters, 79, 397–411.

Connolly, J.W.D., and Haughton, D.R. (1972) The valence of sulfur in glass of basaltic composition formed under low oxidation potential. American Mineralogist, 57, 1515–1517.

Dixon, J.E. (1992) Water and carbon dioxide in basaltic magmas. Ph.D. thesis, California Institute of Technology, Pasadena, California.

Fincham, C.J.B., and Richardson, F.D. (1954) The behaviour of sulfur in silicate and aluminate melts. Proceedings of the Royal Society of London series A, 233, 40–62.

Fornari, D.J., Perfit, M.R., Malahoff, A., and Embley, R. (1983) Geochemical studies of abyssal lavas recovered by DSRV *Alvin* from Eastern Galapagos Rift, Inca Transform, and Ecuador Rift. I. Major element variations in natural glasses and spatial distribution of lavas. Journal of Geophysical Research, 88, 10519–10529.

Frey, F.A., and Clague, D.A. (1983) Geochemistry of diverse basalt types from Loihi Seamount, Hawaii: Petrogenetic implications. Earth and Planetary Science Letters, 66, 337–355.

Gerlach, T.M. (1980) Evaluation of volcanic gas analyses from Kilauea volcano. Journal of Volcanology and Geothermal Research, 7, 295–317.

——— (1993) Oxygen buffering of Kilauea volcanic gases and the oxygen fugacity of Kilauea basalt. Geochimica et Cosmochimica Acta, 57, 795–814.

Haughton, D.R., Roeder, P.L., and Skinner, B.J. (1974) Solubility of sulfur in mafic magmas. Economic Geology, 69, 451–467.

Huebner, J.S., and Sato, M. (1970) The oxygen fugacity-temperature relationships of manganese oxide and nickel oxide buffers. American Mineralogist, 55, 934–952.

Katsura, T., and Nagashima, S. (1974) Solubility of sulfur in some magmas at 1 atm pressure. Geochimica et Cosmochimica Acta, 38, 517–531.

Klein, E., Langmuir, C.H., and Staudigel, H. (1991) Geochemistry of basalts from the Southeast Indian Ridge, 115° to 138°E. Journal of Geophysical Research, 96, 2089–2107.

Kucha, H., Wouters, R., and Arkens, O. (1989) Determination of sulfur and iron valence by microprobe. Scanning Microscopy, 3, 89–97.

Luhr, J.F. (1990) Experimental phase relations of water- and sulfur-saturated arc magmas and the 1982 eruptions of El Chichón volcano. Journal of Petrology, 31, 1071–1114.

Moore, J.G. (1970) Water content of basalt erupted on the ocean floor. Contributions to Mineralogy and Petrology, 28, 272–279.

Moore, J.G., and Schilling, J.G. (1973) Vesicles, water, and sulfur in Reykjanes Ridge basalts. Contributions to Mineralogy and Petrology, 41, 105–118.

Moore, J.G., Batchelder, J.N., and Cunningham, C.G. (1977) CO_2-filled vesicles in mid-ocean ridge basalt. Journal of Volcanology and Geothermal Research, 2, 309–327.

Muenow, D.W., Garcia, M.O., Aggrey, K.E., Bednarz, U., and Schmincke, H.U. (1990) Volatiles in submarine glasses as a discriminant of tectonic origin: Application to the Troodos ophiolite. Nature, 343, 159–161.

Nagashima, S., and Katsura, T. (1973) The solubility of sulfur in Na_2O-SiO_2 melts under various oxygen partial pressures at 1100, 1250, and 1300°C. Bulletin of the Chemical Society of Japan, 46, 3099–3103.

Sakai, H., Casadevall, T.H., and Moore, J.G. (1982) Chemistry and isotope ratios of sulfur in basalts and volcanic gases at Kilauea Volcano, Hawaii. Geochimica et Cosmochimica Acta, 46, 729–738.

Sakai, H., Des Marais, D.J., Ueda, A., and Moore, J.G. (1984) Concentrations and isotope ratios of carbon, nitrogen and sulfur in ocean-floor basalts. Geochimica et Cosmochimica Acta, 48, 2433–2441.

Snyder, D.A., and Carmichael, I.S.E. (1992) Olivine-liquid equilibria and

the chemical activities of FeO, NiO, Fe_2O_3, and MgO in natural basic melts. Geochimica et Cosmochimica Acta, 56, 303–318.

Wallace, P., and Carmichael, I.S.E. (1992a) Sulfur in basaltic magmas. Geochimica et Cosmochimica Acta, 56, 1863–1874.

——— (1992b) Oxidation state of sulfur in submarine glassy lavas as determined by electron microprobe (abs.). Eos, 73, 607.

Wilbur, D.W., and Gofman, J.W. (1965) Chemical bonding and the sulfur *K* X-ray spectrum. Advances in X-ray Analysis, 9, 354–364.

Manuscript received January 28, 1993
Manuscript accepted September 17, 1993

Appendix Table 1. Sample locations, depths of recovery, analytical data, and calculated intensive parameters for Lau Basin glasses

Sample	Latitude	Longitude	Depth	Mg′	FeO	FeO_{tot}	Fe^{3+}/Fe_{tot}	*T* (°C)	Log f_{O_2}	Log f_{S_2}	Log f_{SO_2}
10-1-3	19.14°S	176.53°W	2260	28.8	14.64	17.28	0.153	1089	−9.34	0.35	0.90
12-5-3	18.92°S	176.55°W	2350	33.2	9.34	11.64	0.198	1083	−8.85	0.15	1.37
20-5-1	19.49°S	175.96°W	2640	20.4	9.45	11.72	0.194	1056	−9.14	0.33	1.45
22-6-2	19.69°S	175.99°W	2730	56.5	9.73	10.92	0.109	1181	−9.35	−1.00	−0.66
41-3-2	19.28°S	176.17°W	3050	68.4	7.76	9.08	0.145	1247	−7.87	−0.99	0.27

Note: depth is in meters. Mg′ is the molar ratio $100Mg/(Mg + Fe^{2+})$. FeO determined by colorimetry using a technique of Carmichael (see Christie et al., 1986). FeO_{tot} is Fe_{tot} determined by electron microprobe. Intensive parameters are calculated as described in Wallace and Carmichael (1992a).